scientific reports

Check for updates

OPEN

MOTS-c mimics exercise to combat diabetic liver fibrosis by targeting Keap1-Nrf2-Smad2/3

Feilong Chen, Zhiyu Li, Tutu Wang, Yu Fu, Lei Lyu, Chengyuan Xing, Shunchang Li✉ & Li

Liver fibrosis is a common complication of T2DM(Type 2 diabetes mellitus). Appropriate intervention (exercise or drugs) in the early stage of liver fibrosis can slow down or even reverse liver fibrosis. MOTS-c (Mitochondrial open reading frame of the 12 S r RNA type-c) has been described as an exercise-mimicking substance, and its effects are similar to those achieved by aerobic exercise; however, the exact mechanism remains to be elucidated. In this study, liver function was impaired in a T2DM rat model, leading to the aggravation of liver fibrosis. T2DM rats with liver fibrosis were subjected to MOTS-c, aerobic exercise therapy, or their combination. HE staining, Masson's trichrome staining and immunohistochemistry were used for histopathological examination. Transcriptome sequencing, q-PCR and WB were used to detect the expression of Keap1 (Kelch-like ECH-associated protein 1), Nrf2 (Nuclear factor erythroid 2-related factor 2), Smad2/3/4 and other genes. MOTS-c and aerobic exercise therapy improved T2DM-induced liver fibrosis. Additionally, cells were transfected with MOTS-c overexpression or interference plasmids or MOTS-c was added to the culture medium. MOTS-c overexpression or MOTS-c addition to the culture medium inhibited ROS levels, increased the mRNA and protein expression of Keap1-Nrf2 pathway genes and decreased the expression of TGF-β1(Transforming growth factor-beta1)/Smad pathway genes. Our findings demonstrate that MOTS-c modulates the progression of T2DM complicated by liver fibrosis through a Keap1-Nrf2-Smad2/3 signaling pathway-dependent mechanism.

Keywords MOTS-c, T2DM, Aerobic exercise, Liver fibrosis, Keap1-Nrf2-Smad2/3 pathway

T2DM is a metabolic disease caused by insulin resistance (IR) or insufficient insulin secretion, which reduces the body's ability to regulate blood glucose[1]. The primary causes of mortality in patients with diabetes mellitus are diverse chronic complications. Previous research has focused primarily on renal, cardiovascular, and neurological disorders associated with diabetes mellitus[2]. Little attention has been given to diabetes-induced liver injury, which is primarily attributed to the robust compensatory capacity of the liver and the absence of overt symptoms in early hepatic lesions. As a prevalent complication of T2DM, the prevalence of nonalcoholic fatty liver disease (NAFLD) is steadily increasing[3], and NAFLD has emerged as the primary cause of chronic liver disease globally. NAFLD encompasses a spectrum of hepatic disorders, including hepatic steatosis, nonalcoholic steatohepatitis (NASH), liver fibrosis, cirrhosis, and advanced hepatocellular carcinoma (HCC)[4]. Notably, the incidence of NAFLD in T2DM patients is 47.3–63.7%, and these patients often have liver fibrosis; at least 1/6 of patients with type 2 diabetes have moderate to severe fibrosis (F2 or higher stage), and fibrosis easily develops into cirrhosis and even HCC[5]. Therefore, exploring the pathogenesis of liver fibrosis in T2DM patients complicated with NAFLD is important.

Liver fibrosis is a major liver disease characterized by the accumulation of collagen fibres in the extracellular matrix (ECM). Clinical studies have shown that early liver fibrosis can slowly reverse after removing or controlling pathogenic factors, but liver fibrosis in stage 2 and above patients requires long-term treatment[6]. The activation of hepatic stellate cells (HSCs) is a key link in the development of liver fibrosis[7]. Excess fat can cause oxidative stress in the liver, leading to hepatocyte damage, resulting in the activation of Kupffer cells (KCs) and excessive production of inflammatory cytokines[8]. Liver fibrosis is a response to tissue injury and is accompanied by the accumulation of extracellular matrix (ECM) secreted mainly by HSCs[9]. At present, antifibrotic drugs in clinical use or testing include antioxidants (such as N-acetylcysteine) and anti-inflammatory drugs (such as pirfenidone), but their limited efficacy and relatively obvious side effects limit their wide application[10]. Appropriate interventions (exercise or drugs) after liver fibrosis can slow down or even reverse liver fibrosis[11–13]. Previous studies have shown that aerobic exercise can effectively improve liver fibrosis in NAFLD model mice[14,15],

Sports Medicine Key Laboratory of Sichuan Province, Expert Centre of Sichuan Province, Institute of Sports Medicine and Health, Chengdu Sport University, Chengdu, China. ✉email: lishunchang@cdsu.edu.cn

and moderate aerobic exercise for 150 min/week can reduce early liver injury in T2DM model rats[16], which significantly inhibits liver fibrosis. Liver fibrosis can lead to metabolic dysfunction, and T2DM is a metabolic disease that reduces the body's ability to regulate blood glucose caused by insulin resistance or insulin secretion deficiency. Therefore, aerobic exercise is a way to improve liver fibrosis.

MOTS-c () is a signal molecule encoded by mitochondrial DNA that was discovered in 2015; it contains 16 amino acids and is related to the metabolic regulation of insulin[17,18]. MOTS-c is widely distributed and expressed in various tissues (brain, heart, liver, muscle, testis, kidney, gut, and plasma) in rodents and humans. After the mice were fed, the intraperitoneal injection of MOTS-c significantly reduced the blood glucose level and visceral fat, and the results were similar to those of aerobic exercise. Therefore, MOTS-c is regarded as a sports-mimicking substance[19]. Compared with normal HEK293 cells, HEK293 cells stably overexpressing MOTS-c had significantly reduced long-chain fatty acids and increased fatty acid utilization[20]. It is located mainly in mitochondria in the resting state and is then transferred to the nucleus under the induction of oxidative stress. It can interact with Nrf2 (nuclear factor E2-related factor 2) and participate in antioxidative stress[21–23]. As a typical antioxidative stress pathway, the Keap1 (Kelch-like ECH-associated protein 1)-Nrf2 pathway is activated by high levels of ROS (reactive oxygen species), aerobic exercise or MOTS-c in T2DM[24]. In clinical studies, the expression of MOTS-c is decreased in T2DM patients. In HFD-induced T2DM mice, the TGF-β1/Smad pathway is activated, and liver fibrosis is obvious. In a rat model, MOTS-c can inhibit T2DM and reduce oxidative stress and liver fibrosis[19,25,26].

Previous studies from our group have shown that MOTS-c may treat oxidative stress-induced myocardial ultrastructure damage and cardiac dysfunction by activating the Keap1-Nrf2 signalling pathway and can also modulate antioxidant defence mechanisms during aerobic exercise to reduce diabetic myocardial damage in rat heart tissue[27]. It can also modulate antioxidant defence mechanisms during aerobic exercise and reduce diabetic myocardial injury[27]. Our team also showed that Keap1 can bind to Smad2/3 in HepG2 cells and then modulate Smad2/3 expression through the Keap-Nrf2 pathway[28]. Based on our previous basic research, we hypothesized that MOTS-c could mimic the effects of exercise by improving liver dysfunction in T2DM rats with liver fibrosis. The mechanism may be related to the activation of MOTS-c through the Keap1-Nrf2-Smad2/3 pathway, which activates antioxidative stress in hepatocytes and inhibits liver fibrosis.

Results

MOTS-c and aerobic exercise alleviated liver tissue damage caused by T2DM

To investigate the protective effects of MOTS-c and aerobic exercise on liver tissue in T2DM rats, the rats were treated with exercise, MOTS-C injection or their combination for 8 weeks. Compared with group C (control group), group D (diabetic group)lost weight for 8 weeks, while DE (diabetic MOTS-c group), DM (diabetic MOTS-c group) and DME (diabetic exercise + MOTS-c group) only lost weight in the first 4 weeks, and gradually increased from the fifth week. The body weight of the diabetic (D) group was significantly lower than that of the control (C) group at week 8. Compared with those of the D group, the body weights of the diabetic exercise (DE), diabetic MOTS-c (DM) and diabetic exercise + MOTS-c (DME) groups were significantly greater after the three different treatments (Fig. 1A). Compared with group D, the expression of fasting insulin in DE, DM and DME was significantly improved(Fig. 1B).Additionally, the levels of FBG, HOMA-IRand HbA1c were measured, and the results revealed that aerobic exercise, MOTS-c and their combination effectively reduced their expression compared with that in the D group (Fig. 1C-E).

To explore whether aerobic exercise, MOTS-c and their combination can improve liver function injury caused by diabetes. Therefore, the typical indices of liver function, ALT and AST, were measured. In Group D, the levels of ALT and AST were significantly increased, but after DE, DM and DME treatment, the abnormal increase caused by diabetes was obviously inhibited (Fig. 1F-G). To further explore the effects of MOTS-c and aerobic exercise on improving liver tissue function, we performed HE and Masson assays on liver tissue from each experimental group (Fig. 1H-I). Histopathological analysis revealed distinct morphological differences between the experimental groups. Compared to Group C, Group D exhibited marked hepatocyte vacuolar degeneration, characterized by cytoplasmic vacuoles of varying sizes (blue arrows). Notably, perivascular inflammatory infiltrates were substantially increased in Group D, with only sparse lymphocyte populations observed near blood vessels (purple arrows)(Fig. 1H). However, in the DE, DM, and DME groups, these pathological changes were suppressed, vacuolar degeneration of hepatocytes was reduced (blue arrows), and infiltration of lymphocytes around the blood vessels was not detected compared with that in Group D (Fig. 1H). Compared with those in the C group, the results of Masson's staining revealed that the T2DM group (Group D) presented liver connective tissue hyperplasia with significantly distorted structures and fibrous collagen deposition between the portal vein and the lobules(blue arrows), suggesting that liver fibrosis had formed (Fig. 1I). In contrast, the accumulation of collagen fibres was significantly reduced after treatment with aerobic exercise, MOTS-c, or their combination, suggesting that all three different modalities have a protective effect on liver fibrosis. These results showed that both MOTS-c and aerobic exercise can ameliorate the liver function damage caused by T2DM in rats.

MOTS-C and aerobic exercise modulateliver fibrosis in T2DM rats through the Keap1-Nrf2-Smad2/3 pathway

Transcriptome sequencing is an effective way to screen for differentially expressed genes. Transcriptome sequencing was performed on liver tissues from five groups((C, D, DE, DM and DME group). In the form of a bar chart, differentially expressed genes between different treatment groups are represented: red represents "up", and blue represents "down". As shown in Fig. 2A, compared with those in the C group, 160 genes were upregulated and 99 genes were downregulated in the D group. After the DE, DM and DME groups were compared with Group D, 85, 87 and 67 upregulated genes and 112, 227 and 124 downregulated genes, respectively, were identified. The DM group presented the greatest number of differentially expressed genes (314). Venn diagram

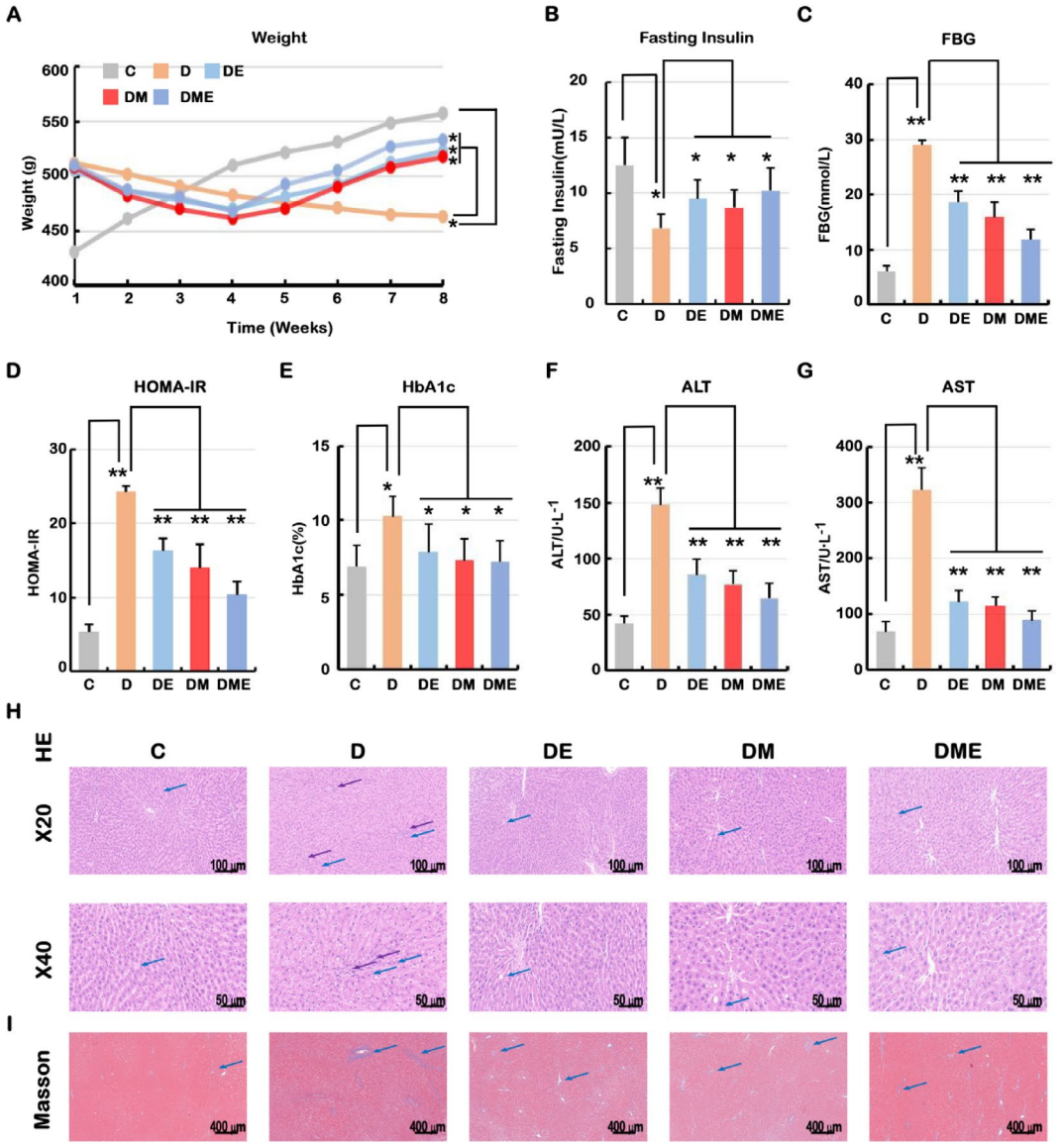

Fig. 1. MOTS-c and aerobic exercise alleviated liver tissue damage caused by T2DM. **(A)** Analytical balance was used to measure the mean body weight of rats in control group (C), diabetic group (D), diabetic exercise group (DE), diabetic MOTS-c group (DM), and diabetic exercise + MOTS-c group (DME). Following confirmation of successful diabetic model establishment after a 7-week high-fat/high-sucrose dietary induction period, longitudinal body weight measurements were conducted weekly throughout the subsequent 8-week experimental phase. **(B)** Fasting insulin was measured in each group.**(C)**Blood samples (0.05 mL) were collected from the tail vein of each group to measure fasting blood glucose (FBG). **(D)** Homeostasis model assessment of insulin resistance (HOMA-IR) was performed as follows: [Plasma glucose (GLU, mmol/L) X serum insulin (m IU/L)]/22.5. **(E)** Blood was collected from the five groups and tested according to the procedure of the HbA1c detection kit. ALT**(F)** and AST **(G)** in the five groups were measured using ELISA kits. HE **(H)** and Masson **(I)** staining were used to detect the pathological changes of liver tissues in the 5 groups (C, D, DE, DM and DME group). All results are given as the mean ± standard deviation (SD). $n = 3$, * $p < 0.05$, ** $p < 0.01$.

analysis revealed 11 common differentially expressed genes (DEGs) (Fig. 2B). Furthermore, through in-depth analysis of transcriptome data, typical antioxidative stress (Keap1-Nrf2 pathway) and fibrosis pathway (TGF-β1-Smad pathway) genes were selected for heatmap analysis, and the results revealed certain differences between each group (Fig. 2C).

The expression of these genes was subsequently verified by q-PCR (Quantitative Polymerase Chain Reaction) and WB(Western Blot). As shown in Fig. 2D, compared with those in Group C, the mRNA expression of *Nrf2*, *Gclc(glutamate cysteine ligase)*, *Gclm(glutamate-cysteine ligase modifier subunit)* and *Ho-1* in Group D decreased, and the mRNA expression of *Keap1*, *Tgf-β1*, *Smad2/3/4*, *Collagen I(Col I)*, *Collagen III(Col III)*, *and α-Sma* increased, and the differences were significant. Compared with those in the D group, the mRNA expression

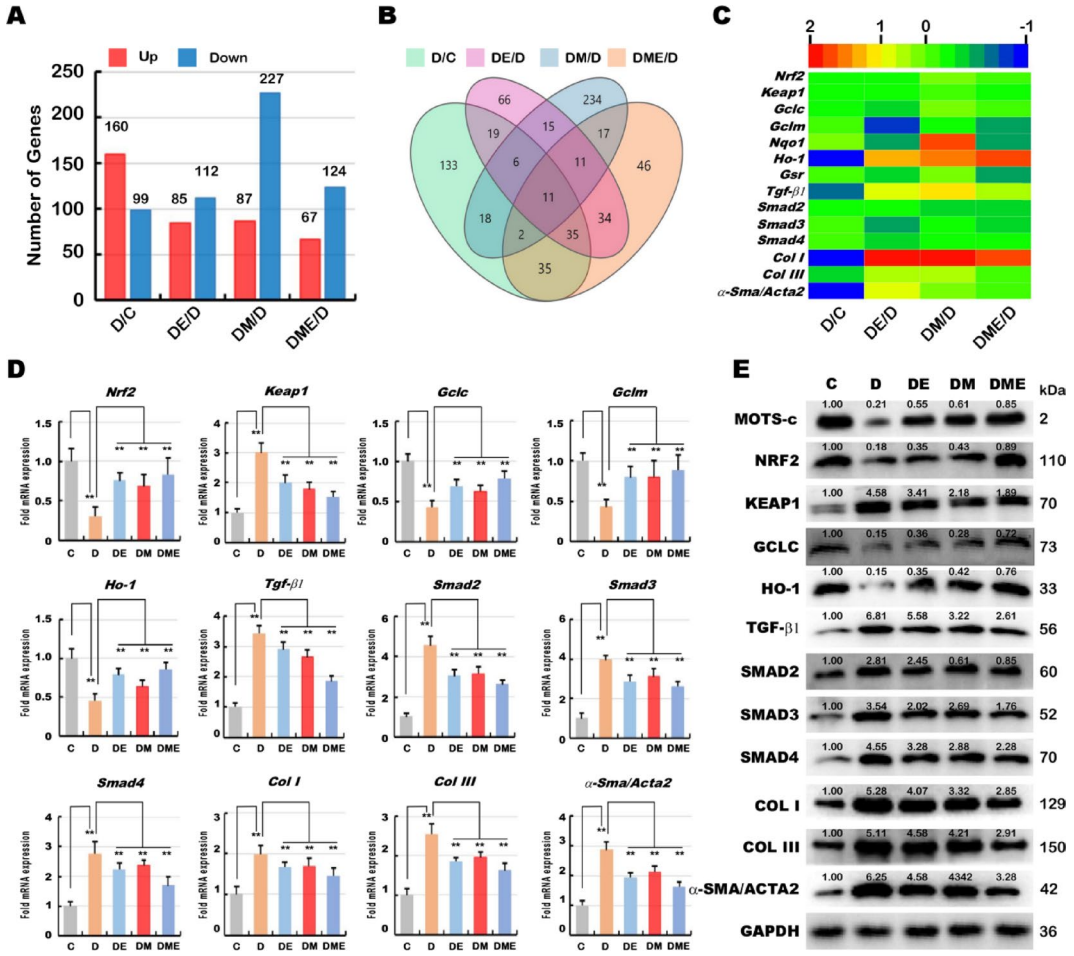

Fig. 2. MOTS-C and aerobic exercise modulate liver fibrosis in T2DM rats through the Keap1-Nrf2-Smad2/3 pathway. By transcriptome sequencing, the differentially expressed genes in the 5 groups (C, D, DE, DM and DME group) were analyzed by bar chart **(A)** and Venn diagram**(B)**. **(C)** Based on transcriptome data, the expression of *Nrf2*, *Keap1*, *Gclm*, *Gclm*, *Ho-1*, *Tgf-β1*, *Smad2/3/4*, *Col I*, *Col III* and *α-Sma* in 5 groups were analyzed by cluster heat map. **(D)** Real-time qPCR was used to quantify the mRNA expression levels of *Nrf2*, *Keap1*, *Gclm*, *Gclm*, *Ho-1*, *Tgf-β1*, *Smad2/3/4*, *Col I*, *Col III* and *α-Sma* in the liver tissue of the five groups. **(E)** Western blotting was employed to determine the protein abundances of MOTS-c, NRF2, KEAP1, GCLC, HO-1, TGF-β1, SMAD2/3/4, COL I, COL III, and α-SMA in the liver tissue of the five groups. The intensity of those immunoblots, representing different protein expression levels, was also quantified by the Quantity One 4.6.2 software, as shown in the figure. The quantitative data was reflected in the numbers above each protein. The larger the number, the higher the gray level.The WB experiment results in the paper came from the same complete gel, but it was cut in the nurturing process to separate the nurturing into different proteins. All results are given as the mean ± standard deviation (SD). $n = 3$, ** $p < 0.01$.

levels of Nrf2, *Gclc*, *Gclm* and *Ho-1* were increased, and the mRNA or protein expression levels of *Keap1*, *Tgf-β1*, *Smad2/3/4*, *Col I*, *Col III*, *and α-Sma* were decreased in the DE, DM and DME groups. The expression of MOTS-c in five rat groups was detected by WB (Fig. 2E). The results showed that the protein expression of MOTS-c in group D was significantly lower than that in group C. Compared with group D, the levels in DE, DM and DME groups were significantly higher. The expression of NRF2, KEAP1,GCLC, HO-1, TGF-β1, SMAD2/3/4, COL I, COL III and α-SMA proteins was also determined. The expression results of the proteins were similar to the mRNA expression trends observed in Fig. 2D.

Finally, as shown in Fig. 3A-G, the expression of *Nrf2*, *Keap1*, *Tgf-β1*, *Smad2*, *Col I*, *Col III*, and *α-Sma* in the 5 groups was determined using immunohistochemistry, and the results were analysed using the histochemistry score (H-score). The H-score was used to analyse the immunohistochemical results of related genes in each experimental group, and the results were consistent with the mRNA and protein expression results. These findings indicate that MOTS-c and aerobic exercise can activate the Keap1-Nrf2-Smad2/3 pathway and the expression of related genes in theliver and modulate the progression of liver fibrosis.

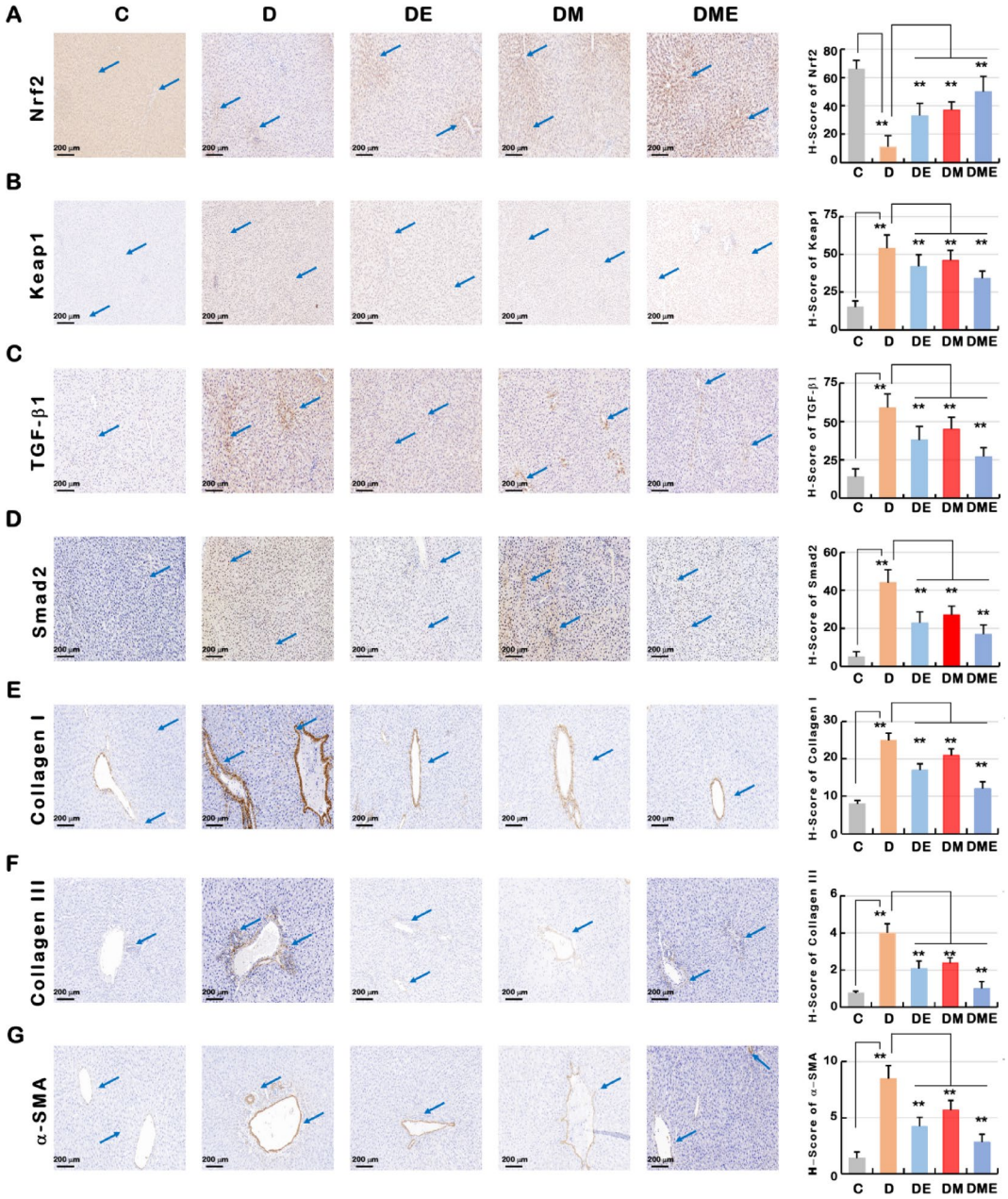

Fig. 3. The expression of intracellular antigen in liver tissue of 5 groups was detected by immunohistochemical method. Immunohistochemistry was used to detect the expression of *Nrf2*(**A**), *Keap1*(**B**), *TGF-β1*(**C**), *Smad2*(**D**), *Col I*(**E**), *Col III*(**F**) and *α-Sma*(**G**) in the liver tissue of the five groups, and the results were analyzed by Histochemistry score (H-score). The area pointed by the arrow was the main positive area.$n = 3$, ** $p < 0.01$.

Both endogenous and exogenous MOTS-c inhibited ROS levels in LX-2, LO-2 and HepG2 cells

In the present study, our previous results showed that aerobic exercise, MOTS-c and their combination effectively improve liver fibrosis in T2DM rats. To explore whether MOTS-c also inhibits liver fibrosis in cells in vitro. We transfected three different MOTS-c interfering RNAs (siRNA-1, siRNA-2 and siRNA-3) into LX-2 (human liver fibrosis cells, HSCs), LO-2 (human normal liver cells) and HeapG2 (human liver cancer cells) cells, respectively, and the results of WB and q-PCR revealed that siRNA-3 had the best interference effect (Fig. 4A). The MOTS-c overexpression plasmid was subsequently transfected into LX-2, LO-2 and HeapG2 cells, and the results in Fig. 4B show that the protein expression of MOTS-c was significantly increased in the three cell lines.

To investigate whether MOTS-c has a protective effect against oxidative stress. We transfected a no-load plasmid (pcDNA3.1), MOTS-c overexpression plasmid or interference plasmid (siRNA-3) into the above cells and measured ROS levels using flow cytometry. The results revealed that ROS levels were inhibited after the overexpression of MOTS-c, and ROS levels were activated after the interference of MOTS-c expression compared with those in the absence of MOTS-c expression (Fig. 4C). Moreover, 10 μM MOTS-c (chemically synthesized

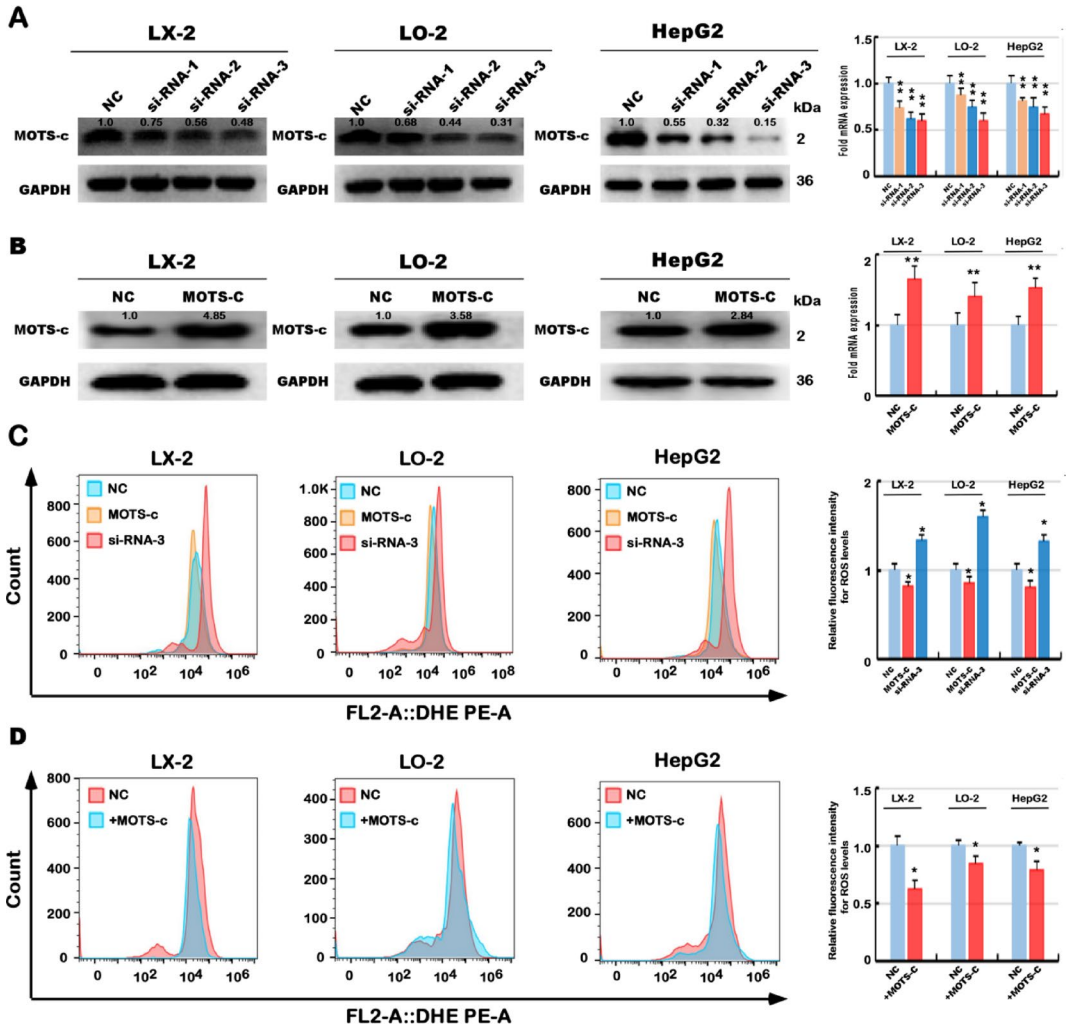

Fig. 4. Both endogenous and exogenous MOTS-c inhibited ROS in LX-2, LO-2 and HepG2 cells. (**A**) We transfected three different MOTS-c interfering RNA (si-RNA-1, si-RNA-2 and si-RNA-3) into LX-2, LO-2 and HeapG2 cells, respectively. The protein abundance of MOTS-c was visualized by Western blotting with indicated antibodies. **(B)** The MOTS-c overexpression plasmid was transfected into LX-2, LO-2 and HeapG2 cells, respectively. Western blotting was employed to determine the protein abundances of MOTS-c. **(C)** After transfection of pcDNA3.1, MOTS-c and si-RNA-3 into cells, the three treatments were named NC group, MOTS-c group and si-RNA-3 group, respectively. ROS was determined by flow cytometry. **(D)** Exogenous MOTS-c was supplemented into the complete culture medium for the cultivation of three distinct cells Cells were divided into two groups according to whether exogenous MOTS-c was added or not: NC group and MOTS-c group (10 μM,24 h). ROS was determined by flow cytometry. The intensity of those immunoblots, representing different protein expression levels, was also quantified by the Quantity One 4.6.2 software, as shown in the figure. The quantitative data was reflected in the numbers above each protein. The larger the number, the higher the gray level.The results were also graphically shown in (C-D), with statistical significances determined by using MANOVA.The WB experiment results in the paper came from the same complete gel, but it was cut in the nurturing process to separate the nurturing into different proteins. $n = 3$, * $p < 0.05$,** $p < 0.01$.

MOTS-c) was added to the culture medium to treat the three cell lines for 24 h. Flow cytometry was used to detect ROS levels. As shown in Fig. 4D, the ROS levels in the three cell lines were significantly lower than those in the NC group (without MOTS-c). In summary, both endogenous and exogenous MOTS-c inhibited ROS levels in the three liver cell lines.

Endogenous MOTS-c inhibited the TGF-β1-SMAD pathway through Nrf2 in LX-2, LO-2 and HepG2 cells

The results in Fig. 4C show changes in the ROS levels after both overexpression and interference with MOTS-c expression in vitro. The KEAP1-NRF2 pathway and its downstream genes are the canonical pathways for antioxidative stress, and our group has previously reported that KEAP1 interacts with Smad2/3[28]. Therefore, we investigated whether the expression of endogenous MOTS-c was inhibited through the KEAP1-NRF2-SMAD2/3 pathway, thereby increasing the antioxidative stress ability of cells. After LX-2 cells were transfected

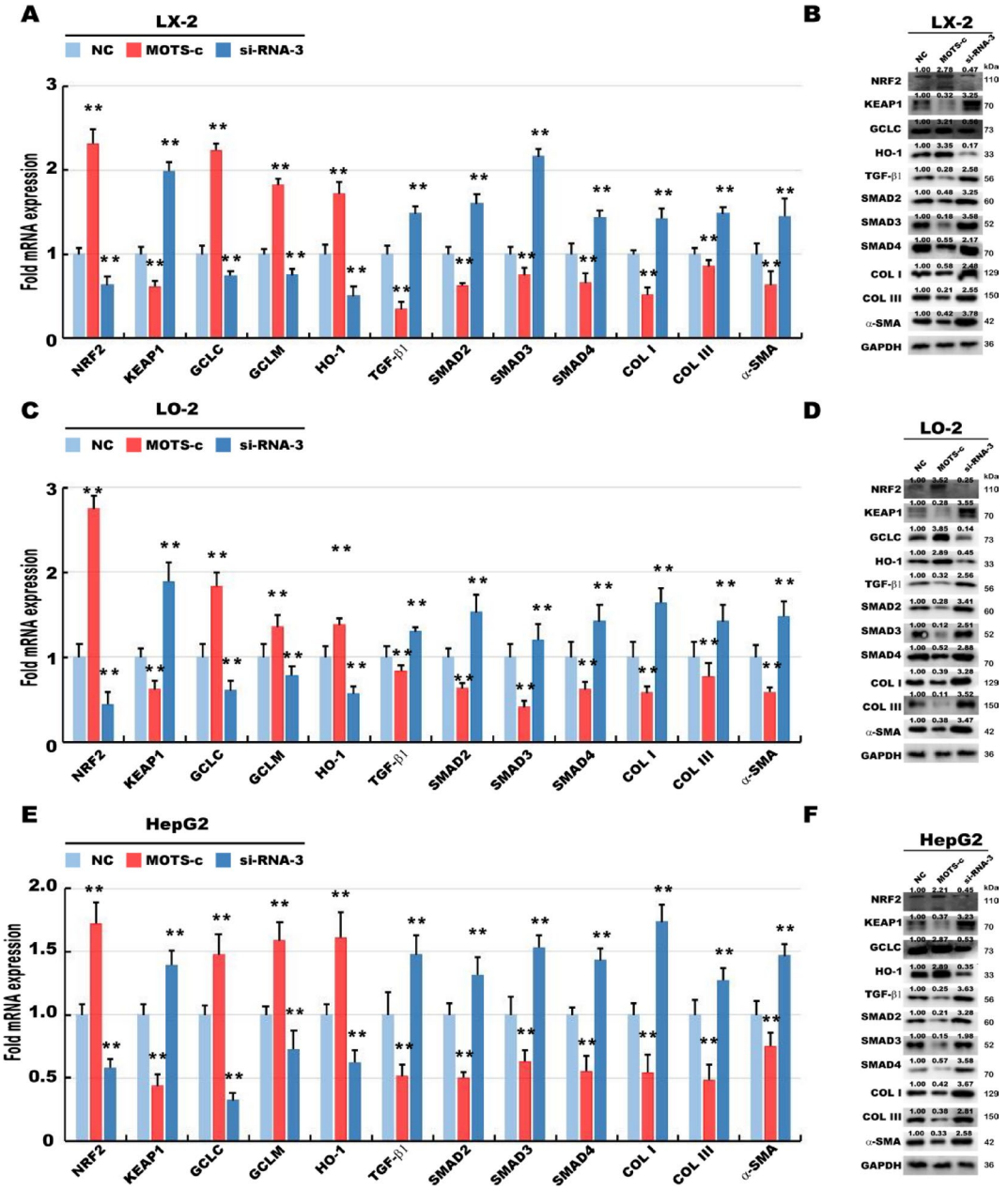

Fig. 5. Endogenous MOTS-c inhibited the expression of TGF-β1-Smads pathway through Nrf2 in LX-2, LO-2 and HepG2 cells. After transfection of pcDNA3.1, MOTS-c and si-RNA-3 into cells, the three treatments were named NC group, MOTS-c group and si-RNA-3 group, respectively. **(A)** Real-time qPCR was used to quantify the mRNA expression levels of *NRF2*, *KEAP1*, *GCLC*, *GCLM*, *HO-1*, *TGF-β1*, *SMAD2/3/4*, *COL I*, *COL III* and *α-SMA* in LX-2 cell lines. **(B)** Western blotting was employed to determine the protein abundances of NRF2, KEAP1, GCLC, HO-1, TGF-β1, SMAD2/3/4, COL I, COL III and α-SMA in LX-2 cell lines. **(C)** The mRNA expression levels of *NRF2*, *KEAP1*, *GCLC*, *GCLM*, *HO-1*, *TGF-β1*, *SMAD2/3/4*, *COL I*, *COL III* and *α-SMA* in LO-2 cell lines were determined by real-time qPCR. **(D)** The protein abundances of NRF2, KEAP1, GCLC, HO-1, TGF-β1, SMAD2/3/4, COL I, COL III and α-SMA in LO-2 cell lines were visualized by Western blotting with indicated antibodies. **(E)** Real-time qPCR was used to quantify the mRNA expression levels of *NRF2*, *KEAP1*, *GCLC*, *GCLM*, *HO-1*, *TGF-β1*, *SMAD2/3/4*, *COL I*, *COL III* and *α-SMA* in HepG2 cell lines. **(F)** Western blotting was employed to determine the protein abundances of NRF2, KEAP1, GCLC, HO-1, TGF-β1, SMAD2/3/4, COL I, COL III and α-SMA in HepG2 cell lines. The intensity of those immunoblots, representing different protein expression levels, was also quantified by the Quantity One 4.6.2 software, as shown in the figure. The quantitative data was reflected in the numbers above each protein. The larger the number, the higher the gray level. The WB experiment results in the paper came from the same complete gel, but it was cut in the nurturing process to separate the nurturing into different proteins. All results are given as the mean ± SD. $n = 3$, ** $p < 0.01$.

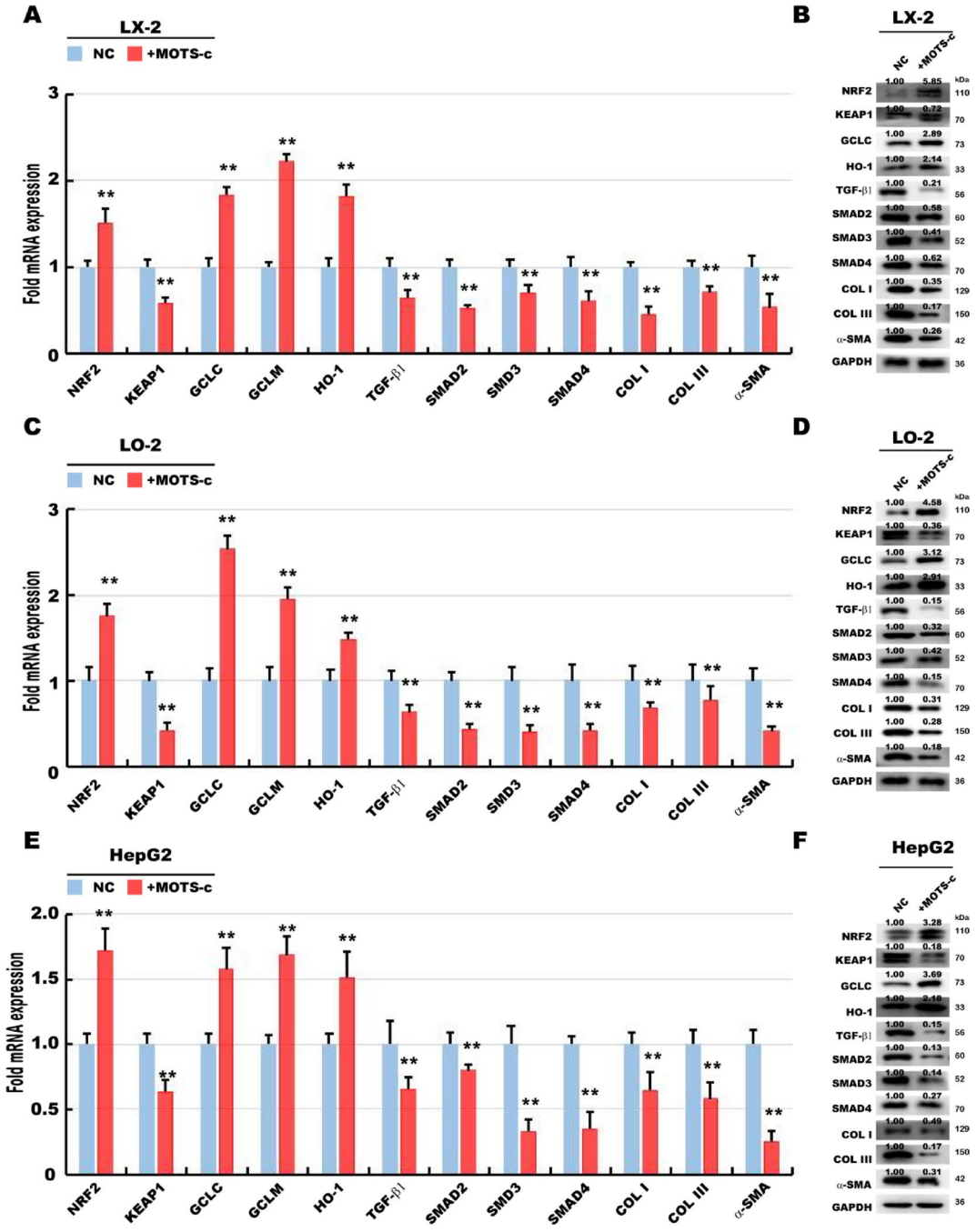

with pcDNA3.1, MOTS-c or siRNA-3, the three treatments were named the NC group, MOTS-c group and siRNA-3 group, respectively. The results of q-PCR and WB revealed that the mRNA or protein expression levels of NRF2, GCLC, GCLM and HO-1 were increased in the MOTS-c group compared with those in the NC group. The mRNA or protein expression levels of KEAP1, TGF-β1, SMAD2/3/4, COL I, COL III and α-SMA were inhibited; however, the results in the siRNA-3 group were completely opposite to those in the MOTS-c group (Fig. 5A-B). In the same manner, the same procedure was performed in LO-2 and HepG2 cells, and the results were consistent with those in LX-2 cells (Fig. 5C-F). These findings suggest that the KEAP1-NRF2-SMAD2/3 pathway can be affected by the expression of endogenous MOTS-c.

Exogenous MOTS-c inhibited the TGF-β1-Smad pathway through Nrf2 in LX-2, LO-2 and HepG2 cells

To explore whether exogenous MOTS-C could modulate the expression of the TGF-β1-Smad2/3 pathway through Nrf2 in cells in vitro. Exogenous MOTS-c was supplemented into the complete culture medium for the cultivation of three distinct cells.LX-2 cells were divided into two groups according to whether exogenous MOTS-c was added: the NC group and MOTS-c group (10 μM; 24 h). The results of q-PCR and WB revealed that the mRNA or protein expression levels of NRF2, GCLC, GCLM and HO-1 in the MOTS-c group were significantly greater than those in the NC group. The mRNA or protein expression levels of KEAP1, TGF-

◀**Fig. 6**. Exogenous MOTS-c inhibited the expression of TGF-β1-Smads pathway through Nrf2 in LX-2, LO-2 and HepG2 cells. Exogenous MOTS-c was supplemented into the complete culture medium for the cultivation of three distinct cells.Cells were divided into two groups according to whether exogenous MOTS-c was added or not: NC group and MOTS-c group (10 μM,24 h). **(A)** Real-time qPCR was used to quantify the mRNA expression levels of *NRF2*, *KEAP1*, *GCLC*, *GCLM*, *HO-1*, *TGF-β1*, *SMAD2/3/4*, *COL I*, *COL III* and *α-SMA* in LX-2 cell lines. **(B)** Western blotting was employed to determine the protein abundances of NRF2, KEAP1, GCLC, HO-1, TGF-β1, SMAD2/3/4, COL I, COL III and α-SMA in LX-2 cell lines. **(C)** The mRNA expression levels of *NRF2*, *KEAP1*, *GCLC*, *GCLM*, *HO-1*, *TGF-β1*, *SMAD2/3/4*, *COL I*, *COL III* and *α-SMA* in LO-2 cell lines were determined by real-time qPCR. **(D)** The protein abundances of NRF2, KEAP1, GCLC, HO-1, TGF-β1, SMAD2/3/4, COL I, COL III and α-SMA in LO-2 cell lines were visualized by Western blotting with indicated antibodies. **(E)** Real-time qPCR was used to quantify the mRNA expression levels of *NRF2*, *KEAP1*, *GCLC*, *GCLM*, *HO-1*, *TGF-β1*, *SMAD2/3/4*, *COL I*, *COL III* and *α-SMA* in HepG2 cell lines. **(F)** Western blotting was employed to determine the protein abundances of NRF2, KEAP1, GCLC, HO-1, TGF-β1, SMAD2/3/4, COL I, COL III and α-SMA in HepG2 cell lines. The intensity of those immunoblots, representing different protein expression levels, was also quantified by the Quantity One 4.6.2 software, as shown in the figure. The quantitative data was reflected in the numbers above each protein. The larger the number, the higher the gray level.The WB experiment results in the paper came from the same complete gel, but it was cut in the nurturing process to separate the nurturing into different proteins. All results are given as the mean ± SD. $n = 3$, ** $p < 0.01$.

β1, SMAD2/3/4, COL I, COL III and α-SMA were significantly decreased (Fig. 6A-B). The same results were obtained for LO-2 and HepG2 cells (Fig. 6C-F). Taken together, these results suggest that the KEAP1-NRF2-SMAD2/3 pathway can be affected by the expression of exogenous MOTS-c.

Discussion

Previous studies have shown that the fibrosis progression rate of T2DM patients is faster than that of nontype 2 diabetes patients, resulting in a higher prevalence rate of middle and late fibrosis[29]. Notably, the risk of death in T2DM patients is greatly increased after liver fibrosis enters the advanced stage[30]. Therefore, slowing or reversing the progression of liver fibrosis is an effective way to reduce the risk of death. Excessive fat can induce oxidative stress in the liver, leading to hepatocyte injury, which leads to the activation of Kupffer cells (KCSs) and the excessive production of inflammatory cytokines. Liver fibrosis is a response to liver tissue damage and is accompanied by the accumulation of extracellular matrix (ECM), which is mainly secreted by HSCs[9]. Therefore, HSC activation and excessive extracellular matrix production are hallmarks of liver fibrosis[31].

MOTS-c, as an "exercise mimetic substance", is seen as a promising strategy for the treatment and prevention of diabetes[32][14]. Moreover, few studies have investigated improvements in patients with T2DM complicated with liver fibrosis. In the present study, rats with T2DM complicated with liver fibrosis were used as the experimental animal model. To explore the protective effect of MOTS-c on T2DM complicated with liver fibrosis via aerobic exercise, MOTS-c and combination therapy were intraperitoneally injected. Our study revealed that intraperitoneal injection of MOTS-c modulates body weight, fasting insulin, FBG, HOMA-IR, and HbA1c in male diabetic rats (Fig. 1A-E), which is also consistent with the results of previous studies[20,33]. The higher the values of serum AST and ALT are, the more severe the liver injury is[34]. We found that the expression of AST and ALT decreased after aerobic exercise, intraperitoneal injection of MOTS-C or their combination (Fig. 1F-G). HE staining and Masson's trichrome staining were used to detect pathological changes in liver tissue from 5 rat models. The results revealed that hepatocyte degeneration, perivascular lymphocyte and granulocyte infiltration, and collagen fibre accumulation were significantly reduced after three treatments (aerobic exercise, MOTS-c, and a combination of the two). These findings suggest that the three different methods can improve liver function to a certain extent (Fig. 1H-I).

The Keap1-Nrf2 pathway has been shown to play an important role in antioxidative stress during liver injury[35]. The Keap1–Nrf2 pathway has been shown to play an important role in antioxidative stress during liver injury[36]. The TGF-β1-Smad signalling pathway is a well-known profibrotic pathway, and its fibrosis genes (such as α-SMA, Col I, and Col III) are abnormally expressed[31,37]. Interestingly, MOTS-c is located mainly in mitochondria in the resting state and is translocated to the nucleus under oxidative stress, where it can interact with Nrf2 and participate in antioxidative stress[23]. Moreover, our team reported that Keap1 interacts with Smad2/3[28].

To further explore the potential mechanisms of MOTS-c as an exercise mimic in preventing and treating T2DM with liver fibrosis. First, transcriptome sequencing was performed on the liver tissues of the rats in the 5 groups (C, D, DE, DM and DME). Common DEGs were identified via histograms and Venn diagrams (Fig. 2A-B). The data were subsequently analysed again, and the differences in the expression of 14 genes (*Nrf2*, *Keap1*, *TGF-β1*, *Smad2/3/4*, *Col I*, *Col III* and *α-Sma*) are displayed in the form of a cluster heatmap (Fig. 2C). Second, the mRNA, protein and immunoexpression of MOTS-c, Keap1, Nrf2, TGF-β1, Smad2 and Col I were verified by q-PCR, WB and immunohistochemistry (Fig. 2D-E, **Fig. 3**). The results showed that both MOTS-c and aerobic exercise could activate the antioxidative stress ability of the Keap1-Nrf2 pathway and reduce the expression of the TGF-β1/Smad pathway in the liver tissue of rats, thereby inhibiting the progression of T2DM complicated with liver fibrosis. In conclusion, the in vivo study revealed that MOTS-c had a similar exercise-mimicking effect as aerobic exercise in improving T2DM with liver fibrosis through the Keap1-Nrf2-Smad2/3 pathway.

To investigate the effect of MOTS-c on the Keap1-Nrf2-Smad pathway in isolated hepatocytes. Three liver lines (LX-2, LO-2 and HepG2) were used for validation. For each cell line, MOTS-c was transfected with the

MOTS-c empty vector, overexpression plasmid or siRNA plasmid. Additionally, ROS levels decreased after MOTS-c overexpression but increased otherwise. When MOTS-c was added to the medium, ROS levels were inhibited compared with those in the NC group. Collectively, these findings demonstrate that MOTS-c attenuates the pathological progression of liver fibrosis in LX-2 cells, LO-2, and HepG2 cells through suppression of ROS generation and subsequent oxidative stress pathways **(Fig. 4)**. Furthermore, we investigated the effect of endogenous MOTS-c on the expression of the KEAP1-NRF2-SMAD2/3 pathway. The MOTS-c empty vector, overexpression plasmid and siRNA plasmid were transfected into three kinds of cells. The results of q-PCR and WB revealed that the mRNA or protein expression levels of NRF2, GCLC, GCLM and HO-1 were increased in the MOTS-c group compared with those in the NC group; moreover, the expression levels of Keap1, TGF-β1, SMAD2/3/4, COL I, COL III and α-SMA were decreased (Fig. 5). Moreover, analysis of the data of the three cell types treated with exogenous MOTS-c, as shown in Fig. 6, revealed the same results as those of the MOTS-c-overexpressing cells, as shown in Fig. 5. Through the above in vitro experiments, the molecular mechanism by which endogenous and exogenous MOTS-c improve liver fibrosis in T2DM patients through the Keap1-Nrf2-Smad2/3 pathway was further elucidated.Although DME group was the most effective in preventing the pathological process of liver fibrosis in T2DM. However, MOTS-c group (DM group) also had a significant effect on improving the pathological process.In conclusion, our findings demonstrate that MOTS-c exerts exercise-mimetic effects comparable to aerobic exercise in ameliorating hepatic fibrosis in T2DM rats. It is expected to be a potential target for the early prevention and treatment of T2DM complicated with liver fibrosis in clinical practice and to provide a theoretical basis.

Our research has certain limitations that should be acknowledged: (1) We did not investigate the improvement effects of various MOTS-c treatment regimens (such as different concentrations, administration routes, and frequencies) on rats with T2DM complicated by liver fibrosis. (2) In this study, we only evaluated the expression of the Keap1-Nrf2-Smad2/3 pathway following si-MOTS-c interference; the expression changes after sh-MOTS-c interference were not determined.

Materials and methods

Experimental materials

Seventy male Sprague-Dawley rats (6 weeks old), each weighing 170–185 g, were purchased from Chengdu Dashuo Experimental Animal Co., Ltd. The rats were housed in the animal room of the Institute of Sports Medicine and Health, Chengdu Sport University (22–25 °C and 40–60% air humidity). The room was well ventilated and had a 12/12-h light-dark cycle. The rats were fed either standard chow or high-fat and high-sugar chow (67% standard chow, 20% sucrose, 10% lard, 2% cholesterol, and 1% sodium cholate; Chengdu Dashuo Experimental Animal Co., Ltd.). After feeding rats with a high-fat and high-sugar diet for 7 weeks, their blood glucose and insulin levels were measured, and the insulin resistance index was calculated. The Ethical Committee of Chengdu University of Physical Education approved the experimental protocol (number: 2023 – 126) and conducted it in accordance with relevant guidelines and regulations. The reporting of our study followed the recommendations of animal research: reporting of in vivo experiments (ARRIVE) guidelines[38]. The animals were anesthetized with sodium pentobarbital(40 mg/kg, ip) before their livers were harvested.

Animal model and experimental groups

The rats were fed in the animal room for 2 weeks to observe whether there was a large difference in individual body weight and death. Ten randomly selected rats that served as the control group (C) were fed the standard diet. The remaining 60 rats were fed a high-fat and high-sugar diet and were used to construct a diabetes model. The construction of the T2DM rat model and its verification methods can be found in an article by our team[27,39]. T2DM model rats were randomly divided into the following four groups (10 rats in each group): diabetic group (D), diabetic exercise group (DE), diabetic MOTS-c group (DM), and diabetic exercise + MOTS-c group (DME).

Aerobic exercise protocol

The Bedford motor model protocol was used to treat DE and DME rats[40]. The treadmill exercise protocol was as follows: 3 days of acclimatization at 15 m/min, after which the treadmill speed was increased to 20 m/min for 60 min/day. The rats were exercised 5 days a week for 8 weeks.

MOTS-c intervention

The rats in the DM group and DME group were intraperitoneally injected with MOTS-c for 8 weeks (0.5 mg/kg/day, 7 days/week, GL Biochem Shanghai Ltd. China)[20]. The rats in groups C and D were injected with the same amount of normal saline (0.5 mg/kg/day) in the same way.

Measurements of weight, blood glucose, insulin and glycated haemoglobin

The body weights of the model rats in each group were determined using an animal weight balance (1000 g range, 0.01 g precision, Shanghai Yuyan Scientific Instrument Co., Ltd.). Blood samples of 0.05 mL were collected from the tail vein of the rats in each treatment group to determine the fasting blood glucose (FBG) levels and blood glucose (NFBG) levels using a blood glucose metre. Blood was collected from the abdominal aortas of rats in each treatment group and centrifuged at 2500 r/min for 10 min to obtain serum, which was stored at -80 °C for later use. Serum fasting insulin (FINS) levels were measured using an ELISA kit (Immuno Way Biotechnology Company, USA). Fasting insulin levels were measured with Elisa kits for rat insulin (Immuno Way, USA) with a plate reader (SpectraMax M5 from Thermo Scientific, USA) at 450 nm. Homeostasis model assessment of insulin resistance (HOMA-IR) was performed as follows: [plasma glucose (GLU, mmol/L) × serum insulin (m IU/L)]/22.5. The steps to determine glycated haemoglobin (HbA1c) were BCA quantification, red blood cell

washing, haemolysate production, acidification, hydrolysis, colour development and counting. The detailed operation steps can be found in the article by Xixi Chen et al.[41].

Analysis of ALT and AST

The serum from five groups(C, D, DE, DM and DME group) was collected. The data were analysed according to the ELISA kit procedure for ALT (alanine transaminase; ab234579; Abcam, Waltham, MA, USA) and AST (aspartate aminotransferase; ab263883; Abcam, Waltham, MA, USA).

Chemicals and antibodies

All the chemicals were of the best quality commercially available. The main antibodies used in this study are listed in Table 1.

Cells, cell culture, and transfection

The LX-2(human hepatic stellate cells, HSC), LO-2(human normal liver cells) and HepG2 (human hepatocellular carcinoma cells) cell lines used in this study were purchased from the Cell Bank of Type Culture Collection of Chinese Academy of Sciences (Shanghai, China). A Lipofectamine 3000 transfection kit (Invitrogen, Shanghai, China) was used to perform transfection experiments, and the specific transfection procedures were performed according to the manufacturer's instructions.

Construction of overexpression and SiRNA interference plasmids

Beijing Qingke Biotechnology Co., Ltd. was responsible for the construction and validation of the MOTS-C overexpression and siRNA interference plasmids. The sequence of the MOTS-c expression plasmid vector for pcDNA3.1 is as follows: ATGAGGTGGCAAGAAATGGGCTACATTTTCTACCCCAGAAAACTACGA. Three sets of siRNA were designed, and the sequences are as follows: siRNA-1: F (5'-3'): GGCAAGAAAUGGGCUAC AU, R (5'-3'): AUGUAGCCCAUUUCUUGCC; siRNA-2: F (5'-3'): GCAAGAAAUGGGCUACAUU, R (5'-3'): AAUGUAGCCCAUUUCUUGC; siRNA-3: F (5'-3'): CAAGAAAUGGGCUACAU, UU, R (5'-3'): AAAUGUAG CCCAUUUCUUG.

HE staining, Masson's trichrome staining and immunohistochemistry

Liver tissue excised from a T2DM rat model of hepatic fibrosis was fixed with paraformaldehyde fixative (Servicebio) for 24 h. Immunohistochemical staining with specific antibodies against Nrf2, Keap1, TGF-β1, Smad2, Collagen I and Collagen III was performed on the liver tissues of the 5 groups, and the results were analysed using the histochemistry score (H-score). Masson's trichrome staining and haematoxylin and eosin (HE) staining were also performed on the tissues. Masson's trichrome staining and HE staining were used for pathological analysis. The reagents and antibodies used in this study were provided by Servicebio, Inc.

Western blotting (WB)

After the experimental cells and liver tissues were washed three times with PBS, the total lysates were used for protein extraction. The total protein extract was immediately denatured at 100 °C for 10 min, then naturally cooled to room temperature and stored at -20 °C until use. The eluted proteins were separated by SDS-PAGE with 8–15% polyacrylamide, followed by immunoblotting experiments with different primary and secondary antibodies.

RNA isolation and quantitative real-time PCR (q-PCR)

Total RNA was extracted from cells and liver tissue using an RNA extraction kit (DP419; Tiangen Biotech Co., Ltd., Beijing, China). A Revert Aid first-strand cDNA synthesis kit (Thermo Fisher Scientific) was subsequently used for reverse transcription.

Antibodies	Identifier	Source
MOTS-c	101AP	FabGennix
NRF2	A0674	ABclonal
KEAP1	ab227828	abcam
GCLC	ab207777	abcam
HO-1	ab189491	abcam
TGF-β1	ab315254	abcam
SMAD2	ab40855	abcam
SMAD3	ab40854	abcam
SMAD4	ab230815	abcam
COL I	ab260043	abcam
COL III	ab184993	abcam
α-SMA/ACTA2	A17910	ABclonal
GAPDH	A19056	ABclonal

Table 1. Main antibody information in the text.

Gene ID	Name	Description	Forward primers(5′-3′)	Reverse Primers (5′-3′)
4549	MOTS-c	human	CAAGAAATGGGCTACATTTTC	GAAAATGTAGCCCATTTCTTG
9817	*KEAP1*	human	CGTGGCTGTCCTCAATCGTCT	CATTGCTGTGATCATTCGCCACT
117,519	*Keap1*	rat	CTCGCAGGATGGTAACCGAACCTT	CCGAAGCTCGTTCATGATGCCAA
4780	*NRF2*	human	GAGAGCCCAGTCTTCATTGCTA	CCGTCTAAATCAACAGGGGCTA
83,619	*Nrf2*	rat	AGTCTTCCATTTACGGAGACCC	ACTGTATCCCCAGAAGAATGTGT
2729	*GCLC*	human	CACCCTCGCTTCAGTACCTT	AATTGCCCATTCCAAATCCCA
25,283	*Gclc*	rat	CCAGACGAAGCCATAAACAAGC	ACAACCTTTTCTCCTCTCCGAT
2730	*GCLM*	human	GTTTGAGACCAGCCTGACCAA	TCTCGGCTCACTGTAACCTC
29,739	*Gclm*	rat	TCAGTCCTTGGAGTTGCACA	CAGTAAGGCTGCAAATGCTC
3162	*HO-1*	human	CAGGCTCCGCTTCTCCGAT	AAGCCAGCCAAGAGAATTCCC
24,451	*Ho-1*	rat	TTCAAACAGCTCTATCGTGCTC	TTAGCCTCTTCTGTCACCCT
7040	*TGF-β1*	human	TGTATTTAAGGACACCCGTGCC	AATGACACAGAGATCCGCAG
59,086	*Tgf-β1*	rat	GGCTTTCGCTTCAGTGCTCA	CCAGGTCACCTCGACGTT
4087	*SMAD2*	human	TACTCTCCAATGTTAACCGAA	TATGTAGTATAAGCGCACTCC
29,357	*Smad2*	rat	GAGACCTTCCATGCGTCACA	CACTCCCCTTCCTATATGCC
4088	*SMAD3*	human	TCCCCGAAAACACTAACTTCC	TCCATCTTCACTCAGGTAGCCA
25,631	*Smad3*	rat	TGCCACTGTCTGCAAGATACCC	TCAAAGCCCTGGTTGACAGACTGA
4089	*SMAD4*	human	AAATATTGTCAGTATGCGTTT	TACTTGATGGAGCATTACTCT
50,554	*Smad4*	rat	TCGCTTTTGCTTGGGTCAACTCT	TCCAACTGCACTCCTTTGCCTA
1277	*COL I*	human	CTGGTACATCAGCAAGAACCCCAA	TACTCGAACTGGAATCCATCGGT
295,532	*Col I*	rat	CTGGTACATCAGCCCAAACCC	GAACCTTCGCTTCCATACTCGAAC
1281	*COL III*	human	TGGAATCTGTGAATCATGCCCTA	TGCGAGTCCTCCTACTGCTA
84,032	*Col III*	rat	ACAAATAGAGAGTCTTATCAGCC	TTCTCCGCTCTTGAGTTCAGG
59	*α-SMA*	human	GGCTGTTTTCCCATCCATTGTG	TCTTTTGCTCTGTGCTTCGTC
81,633	*α-Sma*	rat	TCCCTCTATGCTTCTGGACGTA	CCCTCATAGATAGGCACGTT
2597	*GAPDH*	human	CAACAGCCTCAAGATCATCAGC	TGAGTCCTTCCACGATACCAA
24,383	*Gapdh*	rat	TCAACGGGAAACCCATCACC	TAGACTCCACGACATACTCAGC

Table 2. Primer pairs used for q-PCR analysis.

This cDNAs were used as the template of real-time quantitative PCR (RT-qPCR) with each pair of the indicated gene primers. The primer sequences are listed in Table 2.All these experiments were completed by CFX 96 instrument in Go Taq real-time PCR detection system. The resulting data were analyzed by Bio Rad CFX manager 3.1 software and then presented in graphical form. The comparative CT (ΔΔCt) method was used to calculate the gene expression level.

ROS determination by flow cytometry

To measure intracellular ROS (reactive oxygen species) levels, the same number of cells, 3×10^5 cells in each well of 6-well plates, were seeded and allowed to grow for 24 h. After reaching 80% confluence, the cells were treated with 10 μM MOTS-c for 24 h[42]. The cells were collected according to the procedure of the ROS detection kit, and intracellular ROS levels were detected by flow cytometry.

Transcriptome sequencing

Rat liver tissue samples were subjected to transcriptome sequencing analysis on an Illumina HiSeq 2000 sequencing system (Illumina, San Diego, CA, USA) at the Beijing Genomics Institute (BGI, Shenzhen, China). From the transcriptome data, all of the differentially expressed genes (DEGs) were identified by standard fold changes of ≥ 2 or ≤ 0.5 with an FDR (false discovery rate) of ≤ 0.001 using the Poisson distribution model method (PossionDis) and further analysed in depth as described previously[43,44].

Statistical analysis

IBM SPSS Statistics 22 software was used for statistical analysis. All differences involved in this study were analysed using Student's t-test (comparison between two groups). Relevant data were obtained from at least three independent experiments and are presented as broken line changes. All data were represented as the mean ± SD, relative to the indicated control, with significant differences calculated as values of $p < 0.05$ or 0.01.

Data availability

All of the data is contained within the article. The datasets generated and/or analysed during the current study are available in the National Center for Biotechnology Ifmation and supplementary dataset file.

Received: 7 November 2024; Accepted: 21 May 2025

Published online: 27 May 2025

References

1. Pearson, E. R. Type 2 diabetes: a multifaceted disease. *Diabetologia* **62**, 1107–1112. https://doi.org/10.1007/s00125-019-4909-y (2019).
2. Feldman, E. L. et al. Diabetic neuropathy. *Nat. Rev. Dis. Primers*. **5**, 42. https://doi.org/10.1038/s41572-019-0097-9 (2019).
3. Zheng, Y., Ley, S. H. & Hu, F. B. Global aetiology and epidemiology of type 2 diabetes mellitus and its complications. *Nat. Rev. Endocrinol.* **14**, 88–98. https://doi.org/10.1038/nrendo.2017.151 (2018).
4. Ferguson, D. & Finck, B. N. Emerging therapeutic approaches for the treatment of NAFLD and type 2 diabetes mellitus. *Nat. Rev. Endocrinol.* **17**, 484–495. https://doi.org/10.1038/s41574-021-00507-z (2021).
5. Younossi, Z. M. et al. The global epidemiology of NAFLD and NASH in patients with type 2 diabetes: A systematic review and meta-analysis. *J. Hepatol.* **71**, 793–801. https://doi.org/10.1016/j.jhep.2019.06.021 (2019).
6. Seki, E. & Schwabe, R. F. Hepatic inflammation and fibrosis: functional links and key pathways. *Hepatology* **61**, 1066–1079. https://doi.org/10.1002/hep.27332 (2015).
7. Trautwein, C., Friedman, S. L., Schuppan, D. & Pinzani, M. Hepatic fibrosis: concept to treatment. *J. Hepatol.* **62**, 15–24. https://doi.org/10.1016/j.jhep.2015.02.039 (2015).
8. Kumar, V. et al. Therapeutic targets, novel drugs, and delivery systems for diabetes associated NAFLD and liver fibrosis. *Adv. Drug Deliv Rev.* **176**, 113888. https://doi.org/10.1016/j.addr.2021.113888 (2021).
9. Kumar, V. & Mahato, R. I. Delivery and targeting of MiRNAs for treating liver fibrosis. *Pharm. Res.* **32**, 341–361. https://doi.org/10.1007/s11095-014-1497-x (2015).
10. Wang, P. et al. Promising therapy candidates for liver fibrosis. *Front. Physiol.* **7**, 47. https://doi.org/10.3389/fphys.2016.00047 (2016).
11. Ezpeleta, M. et al. Effect of alternate day fasting combined with aerobic exercise on non-alcoholic fatty liver disease: A randomized controlled trial. *Cell Metab* 35, 56–70 e53 (2023). https://doi.org/10.1016/j.cmet.2022.12.001
12. Miranda, W. R., Kamath, P. S., Jain, C. C., Connolly, H. C. & Egbe, A. C. Liver fibrosis scores are associated with resting and exercise Fontan and pulmonary artery wedge pressures: insights into FALD. *Can. J. Cardiol.* **39**, 1349–1357. https://doi.org/10.1016/j.cjca.2023.04.024 (2023).
13. Houttu, V. et al. Does aerobic exercise reduce NASH and liver fibrosis in patients with non-alcoholic fatty liver disease? A systematic literature review and meta-analysis. *Front. Endocrinol. (Lausanne)*. **13**, 1032164. https://doi.org/10.3389/fendo.2022.1032164 (2022).
14. van den Hoek, A. M. et al. Diet and exercise reduce pre-existing NASH and fibrosis and have additional beneficial effects on the vasculature, adipose tissue and skeletal muscle via organ-crosstalk. *Metabolism* **124**, 154873. https://doi.org/10.1016/j.metabol.2021.154873 (2021).
15. Kawanishi, N. et al. Exercise training attenuates hepatic inflammation, fibrosis and macrophage infiltration during diet induced-obesity in mice. *Brain Behav. Immun.* **26**, 931–941. https://doi.org/10.1016/j.bbi.2012.04.006 (2012).
16. Uslu, S., Alaca, N., Kilic, K. D., Uysal, A. & Kurtel, H. The effects of aerobic exercise frequencies on liver fibrosis, alpha-fetoprotein and cytokeratin 19 in experimental type 2 diabetes-induced rats: an immunohistochemistry study. *Biotech. Histochem.* **93**, 615–622. https://doi.org/10.1080/10520295.2018.1517898 (2018).
17. Kong, B. S., Lee, C. & Cho, Y. M. Mitochondrial-Encoded peptide MOTS-c, diabetes, and Aging-Related diseases. *Diabetes Metab. J.* **47**, 315–324. https://doi.org/10.4093/dmj.2022.0333 (2023).
18. Gao, Y. et al. MOTS-c functionally prevents metabolic disorders. *Metabolites* **13** https://doi.org/10.3390/metabo13010125 (2023).
19. Li, S. et al. MOTS-c and exercise restore cardiac function by activating of NRG1-ErbB signaling in diabetic rats. *Front. Endocrinol. (Lausanne)*. **13**, 812032. https://doi.org/10.3389/fendo.2022.812032 (2022).
20. Lee, C. et al. The mitochondrial-derived peptide MOTS-c promotes metabolic homeostasis and reduces obesity and insulin resistance. *Cell. Metab.* **21**, 443–454. https://doi.org/10.1016/j.cmet.2015.02.009 (2015).
21. Chen, F., Xiao, M., Hu, S. & Wang, M. Keap1-Nrf2 pathway: a key mechanism in the occurrence and development of cancer. *Front. Oncol.* **14**, 1381467. https://doi.org/10.3389/fonc.2024.1381467 (2024).
22. Xiao, J. et al. The Mitochondrial-Derived peptide (MOTS-c) interacted with Nrf2 to defend the antioxidant system to protect dopaminergic neurons against rotenone exposure. *Mol. Neurobiol.* **60**, 5915–5930. https://doi.org/10.1007/s12035-023-03443-3 (2023).
23. Yin, Y. et al. The mitochondrial-derived peptide MOTS-c relieves hyperglycemia and insulin resistance in gestational diabetes mellitus. *Pharmacol. Res.* **175**, 105987. https://doi.org/10.1016/j.phrs.2021.105987 (2022).
24. Fasipe, B., Li, S. & Laher, I. Exercise and vascular function in sedentary lifestyles in humans. *Pflugers Arch.* **475**, 845–856. https://doi.org/10.1007/s00424-023-02828-6 (2023).
25. Arboatti, A. S. et al. Diethylnitrosamine enhances hepatic tumorigenic pathways in mice fed with high fat diet (Hfd). *Chem. Biol. Interact.* **303**, 70–78. https://doi.org/10.1016/j.cbi.2019.02.024 (2019).
26. Ramanjaneya, M. et al. Mitochondrial-Derived peptides are down regulated in diabetes subjects. *Front. Endocrinol. (Lausanne)*. **10**, 331. https://doi.org/10.3389/fendo.2019.00331 (2019).
27. Tang, M. et al. The role of MOTS-c-mediated antioxidant defense in aerobic exercise alleviating diabetic myocardial injury. *Sci. Rep.* **13**, 19781. https://doi.org/10.1038/s41598-023-47073-0 (2023).
28. Chen, F. et al. A novel crosstalk between Nrf2 and Smad2/3 bridged by two nuanced Keap1 isoforms with their divergent effects on these distinct family transcription factors. *Free Radic Biol. Med.* **213**, 190–207. https://doi.org/10.1016/j.freeradbiomed.2024.01.025 (2024).
29. Huang, D. Q. et al. Fibrosis Progression Rate in Biopsy-Proven Nonalcoholic Fatty Liver Disease Among People With Diabetes Versus People Without Diabetes: A Multicenter Study. *Gastroenterology* 165, 463–472 e465 (2023). https://doi.org/10.1053/j.gastro.2023.04.025
30. Sanyal, A. J. et al. Prospective study of outcomes in adults with nonalcoholic fatty liver disease. *N Engl. J. Med.* **385**, 1559–1569. https://doi.org/10.1056/NEJMoa2029349 (2021).
31. Song, Y. et al. Tyrosine kinase receptor B attenuates liver fibrosis by inhibiting TGF-beta/SMAD signaling. *Hepatology* **78**, 1433–1447. https://doi.org/10.1097/HEP.0000000000000319 (2023).
32. Yang, B. et al. MOTS-c interacts synergistically with exercise intervention to regulate PGC-1alpha expression, attenuate insulin resistance and enhance glucose metabolism in mice via AMPK signaling pathway. *Biochim. Biophys. Acta Mol. Basis Dis.* **1867**, 166126. https://doi.org/10.1016/j.bbadis.2021.166126 (2021).
33. Lu, H. et al. MOTS-c peptide regulates adipose homeostasis to prevent ovariectomy-induced metabolic dysfunction. *J. Mol. Med. (Berl).* **97**, 473–485. https://doi.org/10.1007/s00109-018-01738-w (2019).
34. Aljobaily, N. et al. Creatine alleviates Doxorubicin-Induced liver damage by inhibiting liver fibrosis, inflammation, oxidative stress, and cellular senescence. *Nutrients* **13** https://doi.org/10.3390/nu13010041 (2020).
35. Cheng, D. et al. alpha-Ketoglutarate prevents hyperlipidemia-induced fatty liver mitochondrial dysfunction and oxidative stress by activating the AMPK-pgc-1alpha/Nrf2 pathway. *Redox Biol.* **74**, 103230. https://doi.org/10.1016/j.redox.2024.103230 (2024).
36. Galicia-Moreno, M. et al. Roles of Nrf2 in liver diseases: molecular, Pharmacological, and epigenetic aspects. *Antioxid. (Basel)*. 9. https://doi.org/10.3390/antiox9100980 (2020).

37. Budi, E. H., Schaub, J. R., Decaris, M., Turner, S. & Derynck, R. TGF-beta as a driver of fibrosis: physiological roles and therapeutic opportunities. *J. Pathol.* **254**, 358–373. https://doi.org/10.1002/path.5680 (2021).
38. Kilkenny, C. et al. Animal research: reporting in vivo experiments: the ARRIVE guidelines. *Br. J. Pharmacol.* **160**, 1577–1579. https://doi.org/10.1111/j.1476-5381.2010.00872.x (2010).
39. Wang, M. et al. MOTS-c repairs myocardial damage by inhibiting the CCN1/ERK1/2/EGR1 pathway in diabetic rats. *Front. Nutr.* **9**, 1060684. https://doi.org/10.3389/fnut.2022.1060684 (2022).
40. Bedford, T. G., Tipton, C. M., Wilson, N. C., Oppliger, R. A. & Gisolfi, C. V. Maximum oxygen consumption of rats and its changes with various experimental procedures. *J. Appl. Physiol. Respir Environ. Exerc. Physiol.* **47**, 1278–1283. https://doi.org/10.1152/jappl.1979.47.6.1278 (1979).
41. Chen, X. et al. d-Ribose as a contributor to glycated haemoglobin. *EBioMedicine* **25**, 143–153. https://doi.org/10.1016/j.ebiom.2017.10.001 (2017).
42. Zhang, Y. et al. The Mitochondrial-Derived peptide MOTS-c alleviates radiation pneumonitis via an Nrf2-Dependent mechanism. *Antioxid. (Basel)*. 13. https://doi.org/10.3390/antiox13050613 (2024).
43. Chen, F. et al. Different Inhibition of Nrf2 by two Keap1 isoforms alpha and beta to shape malignant behaviour of human hepatocellular carcinoma. *Int. J. Mol. Sci.* **23** https://doi.org/10.3390/ijms231810342 (2022).
44. Audic, S. & Claverie, J. M. The significance of digital gene expression profiles. *Genome Res.* **7**, 986–995. https://doi.org/10.1101/gr.7.10.986 (1997).

Acknowledgements
We thank all other present and pastmembers of Li's laboratory (at Chengdu Sport University, China) for giving critical discussion and invaluable help with this work. We also acknowledge assistance from medical writers, proof-readers and editors.

Author contributions
F.C. performed the experiments with help of Z.L, T.W., Y.F. L.L. and C.X, collected all the relevant data, and wrote the first draft of this manuscript with most figures and supplemental information. S.L. designed and supervised this study, analysed all the data, helped to prepare all figures with cartoons, rewrote and revised the paper. All authors have read and agreed to the published version of the manuscript.

Funding
The author(s) declare that financial support was received for there search, authorship, and/or publication of this article. This work was supported by Natural Science Foundation of Sichuan (2024NSFSC1228), the China Postdoctoral Science Foundation (Certificate Number 2023M740381), the Postdoctoral Fellowship Program (Grade B) of China Postdoctoral Science Foundation under Grant Number GZB20240083, Key Laboratory of Sports Medicine of Sichuan Province (2024-A024) and School of Sports Medicine and Health/Institute of Sports Medicine and Health, Chengdu Sport University 2024–2025 'Excellent Scientific Research Program' (Project No. ZYGH2402).

Declarations

Competing interests
The authors declare no competing interests.

Supplementary Information
All of the data is contained within the article and the supplementary materials.

Additional information
Supplementary Information The online version contains supplementary material available at https://doi.org/10.1038/s41598-025-03526-2.

Correspondence and requests for materials should be addressed to S.L.

Reprints and permissions information is available at www.nature.com/reprints.

Publisher's note Springer Nature remains neutral with regard to jurisdictional claims in published maps and institutional affiliations.